



Visualization of microaneurysms using optical coherence tomography angiography: comparison of OCTA en face, OCT B-scan, OCT en face, FA, and IA images

Masafumi Hamada^{1,2} · Kishiko Ohkoshi² · Keiji Inagaki^{1,2} · Nobuyuki Ebihara^{1,3} · Akira Murakami¹

Received: 8 August 2017 / Accepted: 20 December 2017 / Published online: 30 January 2018
© Japanese Ophthalmological Society 2018, corrected publication February 2018

Abstract

Purpose To compare the visualization of microaneurysms (MAs) in patients with diabetic retinopathy (DR) using optical coherence tomography angiography (OCTA) with that using fluorescein angiography (FA).

Study design Prospective, clinical, and experimental.

Methods This study was a prospective evaluation of imaging technology. Thirty-seven eyes of 33 patients with DR were scanned using an OCTA instrument. The 83 MAs that were confirmed on OCT B-scan and OCT en face images were evaluated using OCTA, and these findings were compared with those evaluated using FA.

Results Of the 83 MAs confirmed on OCT B-scan images, 73 (88%) were clearly visualized on the OCTA en face images as nodular or comma-shaped structures, while the remaining 12% did not present with a typical MA or vascular structure on the OCTA en face images at the relevant positions. Seventy-four of the 83 MAs (87%) confirmed on the OCT B-scan images presented as punctate hyperfluorescent spots on the FA images. On the FA images, 8 of 9 (88%) MAs absent on the OCTA en face images presented as hyperfluorescent spots. Visualization of the MAs on the OCTA en face images did not correlate with the OCT B-scan images of the MA lumens (open, closed, or heterogeneous).

Conclusions For diabetic maculopathy, OCTA en face images do not present with comprehensive MAs images, indicating that some MAs might be overlooked with OCTA en face images.

Keywords Angiography · Diabetic macular edema · Microaneurysms · Optical coherence tomography

Introduction

Recent advances in optical coherence tomography (OCT) have made it possible to evaluate the fine structure of retinal tissue, which has led to marked advances in the understanding of macular disease pathology [1]. Recently, software

loaded onto en face OCT has allowed the observation of the structure of the vascular and capillary network, termed optical coherence angiography (OCTA). Using an image processing method called the split-spectrum amplitude-decorrelation angiography algorithm, images of vascular pathways can now be obtained noninvasively, similarly to those obtained by fluorescein angiography (FA) after intravenous dye injection [2–11].

Recently, several studies have assessed the effectiveness of OCTA in visualizing retinal vascular lesions [12–15]. In 2015, Ishibazawa and colleagues [3] used OCTA to observe the capillary structure of eyes of patients with diabetic retinopathy (DR). They reported that the nonperfusion area (NPA), neovascularization, and MAs were well visualized using en face OCTA. However, they also reported some discrepancies between FA and OCTA. The OCTA en face images did not always depict the punctate hyperfluorescent spots seen in the FA images, particularly MAs [16]. Thus,

The original version of this article was revised: In the original publication, the yellow circles in Figures 2a, 2b, 3a and 3b were placed incorrectly. The figures are corrected.

✉ Masafumi Hamada
hamamasa@luke.ac.jp

¹ Department of Ophthalmology, Juntendo University Graduate School of Medicine, Tokyo, Japan

² Department of Ophthalmology, St. Luke's International Hospital, 9-1 Akashi-cho, Chuo-ku, Tokyo 104-8560, Japan

³ Department of Ophthalmology, Juntendo University Urayasu Hospital, Urayasu, Japan

the reliability of the interpretation of OCTA en face imaging findings, particularly for detecting MAs, remains in question.

Horii and colleagues [17] reported that MAs have characteristic capsular shapes, with ring- or oval-shaped margins, called the ring sign in OCT B-scan tomographic images. OCT B-scan images provide the real image of the MAs themselves, which may be a more reliable detection method than FA or color fundus photography. To detect real MA images, we defined MAs as structures visualized on OCT B-scan images as a capsular image, as described by Horii and colleagues [17]. The purpose of this study was to evaluate the effectiveness of OCTA en face images for detecting MAs by clarifying the discrepancies between OCTA, OCT B-scan, FA, and indocyanine green angiography (IA) images.

Participants and methods

This was a prospective observational study conducted between July and September 2015 with the approval of the St. Luke's International Hospital ethics committee (15-R039). The study adhered to the tenets of the Declaration of Helsinki, and informed consent was obtained from all the study participants.

The inclusion criterion was the presence of macular edema with diabetic maculopathy during the study period. Macular edema was defined as a central macular thickness of 300 μm or more using a Cirrus HD-OCT device (Carl Zeiss Meditec, Jena, Germany) in macular cube 200×200 mode. The exclusion criteria were patients in whom fundus photographs could not be taken because of cloudy ocular media or small pupils; patients who had other retinal vascular diseases; patients with a history of intraocular surgeries; patients treated with direct photocoagulation of the MA, grid photocoagulation, and/or panretinal photocoagulation for DR within the previous 3 months; and patients who did not give consent. We also excluded OCTA images with a signal strength index of 50 or lower.

The participants underwent tests for visual acuity and intraocular pressure, color fundus photography, and en face OCTA (RTVue XR Avanti; Optovue, Fremont, CA, USA) to detect MAs. The following items were also evaluated: age, sex, diabetes stage, disease duration, and the presence or absence of therapeutic interventions for DR. We used color fundus photography and OCT en face images confirmed with OCT B-scans to detect MAs. Then, we obtained FA/IA images of the MAs confirmed by the OCT B-scans to detect hyperfluorescent spots. The FA/IA images were taken within 1 month of the OCTA. The FA/IA device used was the Spectralis (Heidelberg Engineering, Heidelberg, Germany).

OCTA was performed in a 3×3 -mm range that included the fovea in the AngioVue mode. In addition, several fundus

photographs were taken at 3-mm angle views near the fovea in areas where MAs were clearly present, such as areas with multiple red dots or the inside of the circinate ring.

Since MAs were obtained using color fundus photographs and the FA images were not always true, we defined MAs according to the typical MA structure visualized in OCT B-scan images. To detect MAs, we obtained OCT en face images of the entire retinal depth in a 3×3 -mm range, and nodular MAs were observed using the RTVue XR Avanti. MAs were scanned using horizontal and vertical OCT B-scans. Each MA on the OCT en face images was observed using the OCTA en face vascular image and then confirmed using the horizontal and vertical OCT B-scan images simultaneously displayed on a single monitor. The horizontal and vertical sliders were aligned with punctate foci (areas thought to be MAs) and observed in the OCT en face images. Horizontal and vertical OCT B-scan tomograms of these areas were then evaluated to confirm the presence of MAs. MAs were identified in the OCT B-scan images as having characteristic capsular shapes and ring-signs, as described by Horii and colleagues [17] and by Ishibazawa and colleagues [3] (Fig. 1–Fig. 3).

OCTA en face images of MAs with nodular, saccular, or fusiform characteristics were obtained from the images at exactly the same region where the horizontal and vertical sliders were aligned on MAs confirmed using OCT en face and OCT B-scan images [18, 19]. The depth of the AngioVue images was varied to search for MAs from multiple angles. The maximum diameter and depth of the MA confirmed using OCT B-scan images were measured using the scale function on the Optovue RTVue Avanti. Depth was measured as the distance from the inner limiting membrane (ILM) to the center of the MA on OCT B-scan images.

In the OCT B-scan images, MA lumens with low reflectivity were defined as “open,” those with uniform hyperreflectivity were defined as “closed,” and those with heterogeneous reflectivity were defined as “heterogeneous.”

The OCT readings and measurements were confirmed by 2 retinal specialists (K.O., M.H.) with at least 7 years of experience in interpreting OCT results, after masking the clinical findings.

The Wilcoxon signed rank test was used to compare the morphology of the MAs in the OCT en face and/or OCTA en face images, FA findings, IA findings, scale of MAs (OCT B-scan), depth (OCT B-scan), and presence of circinate hard exudates around the MAs. SPSS software version 19.0 (SPSS, Chicago, IL, USA) was used for the statistical analyses. All probability values less than 0.05 were considered significant.

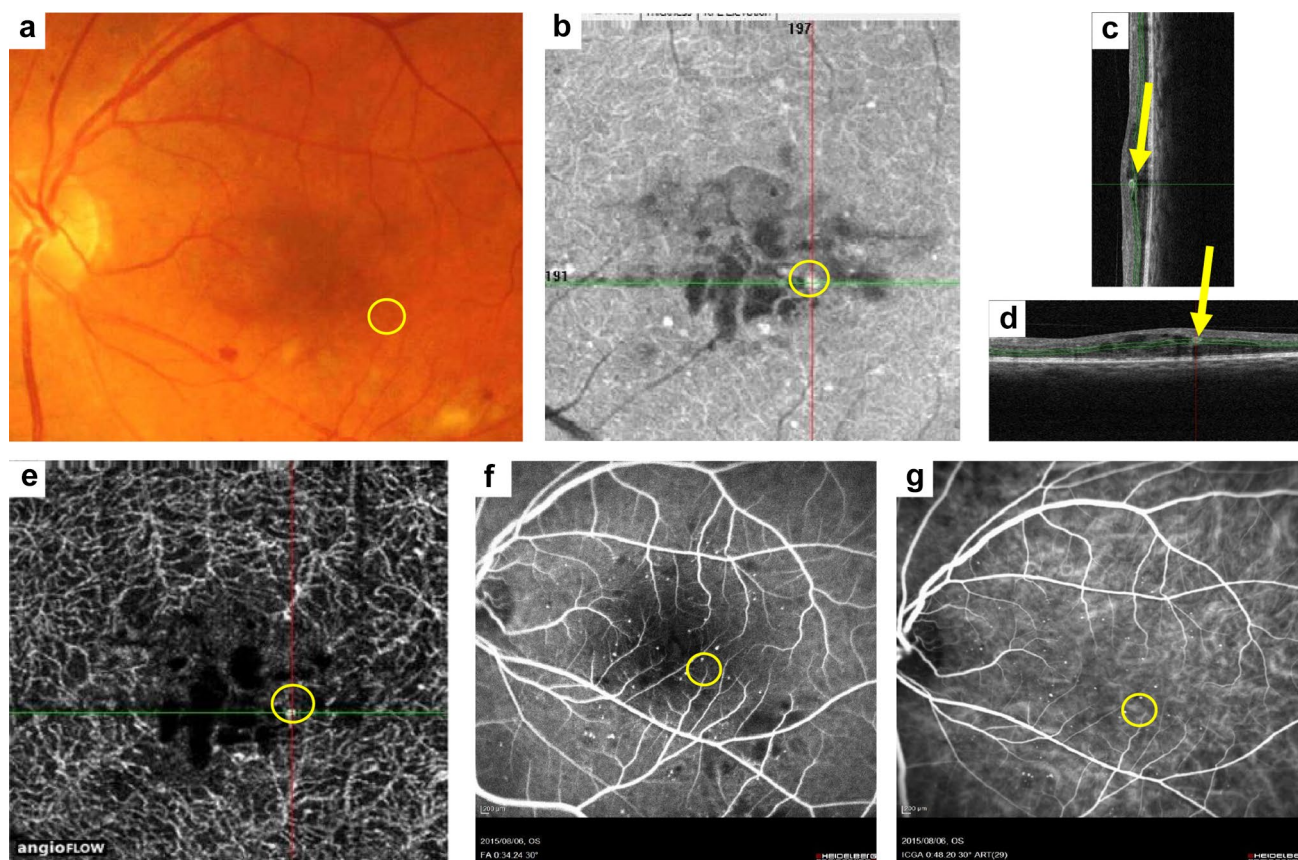


Fig. 1 A 63-year-old man with proliferative diabetic retinopathy of the right eye. **a** The fundus photograph shows a red punctate spot thought to be a microaneurysm (MA; yellow circle). **b** The MA is seen in a 3×3 -mm square of an optical coherence tomography (OCT) en face image (yellow circle). The MA was confirmed in OCT B-scan images with the **c** vertical and **d** horizontal sliders aligned. A ring-shape, thought to be the MA, can be seen. The MA lumen was open and cystoid macular edema was observed in the vicinity. **e**

A nodular finding is seen in a 3×3 -mm square OCT angiography (OCTA) en face image (deep plexus). This was defined as a nodular-type MA. **f** The yellow circle shows hyperfluorescence in a fluorescein angiography (FA) image (34 seconds) matching the OCTA en face image. **g** The yellow circle shows hyperfluorescence in an indocyanine green angiographic (IA) image (48 seconds) matching the OCTA en face image

Results

A total of 49 eyes of 45 consecutive diabetic macular edema (DME) patients who were under outpatient retinal care at our hospital and who agreed to participate in the study were considered for inclusion in the study. Eventually, 37 eyes of 33 patients whose OCTA en face images of MA areas were obtained at a signal strength index of 50 or higher and were of a quality suitable for analysis were included. These eyes comprised 23 eyes of 21 men and 14 eyes of 12 women. The patients' mean (SD) age was 62.4 years (7.5 years) and the mean (SD) disease duration was 40.2 months (41.6 months). In terms of disease stage, 1 eye (3%) had mild, nonproliferative diabetic retinopathy (NPDR); 16 eyes (43%) had moderate NPDR; 8 eyes (22%) had severe NPDR; and 12 eyes (32%) had proliferative diabetic retinopathy (PDR).

Twenty-nine of the 37 patients (78%) had histories of direct MA photocoagulation, grid photocoagulation, and/or panretinal DR photocoagulation more than 3 months before the study. Using the methods described above, we confirmed a total of 83 MAs. A mean 2.26 MAs (1-7 MAs) were confirmed per OCT en face image (3×3 mm).

Seventy-five open (62%), 21 closed (23%), and 3 heterogeneous (4%) MA lumens were found during the OCT B-scans. Cystoid macular edema was observed adjacent to 62 MAs (75%) and was not observed in 21 MAs (25%).

For a stratified analysis of the OCT en face images, the area from $3 \mu\text{m}$ beneath the ILM to $15 \mu\text{m}$ beneath the inferior border of the inner plexiform layer (IPL) was defined as the superficial plexus, and the area 15 to $70 \mu\text{m}$ from the inferior border of the IPL, as the deep plexus. Most MAs were found in the deep plexus, with 74 (90%) in this area and 9 (10%) in the superficial plexus.

The MA depth ranged from 54 μm to 326.5 μm from the ILM (mean, 151.3 μm). The MA diameter ranged from 39 μm to 219 μm (mean, 104.6 μm).

In the OCTA en face images, MAs were visualized in a variety of shapes: nodular, coil-shaped, comma-shaped, semilunar, crescent, and earlobe-like. In addition, some MAs were not visualized on the OCTA en face images. Those MAs were not vascular structures seen at the same positions as MAs confirmed by the OCT B-scan images, despite being clearly visible on the OCT en face and horizontal and vertical OCT B-scan images (10 of the 83 MAs, 12%).

We classified MAs according to shape as follows: nodular type, comma-like type, and absent type. MAs that were visible as nodular findings on OCTA en face images were defined as the nodular type, those that were neither nodular nor absent (coil-shaped, comma-shaped, semilunar, crescent, or earlobe-like) were defined as the comma-like type, and those that could not be confirmed on OCTA en face images were defined as the absent type. There were 54 nodular types (65%), 19 comma-like types (23%), and 10 absent types (12%). Of the comma-like types, MAs presenting comma-like shapes were the most common (16, 85%); additionally, there was 1 semilunar (5%), 1 crescent (5%), and 1 earlobe-like (5%) type.

FA images of the same area were obtained for 74 of the 83 MAs (87%). Sixty-nine of the 74 MAs (93%) that were confirmed using en face and OCT B-scan images presented as punctate hyperfluorescent spots, characteristic of MAs in FA images. Matching hyperfluorescent spots were not observed in the FA images for 5 of the 74 MAs (7%).

Similarly, 24 of the 49 MAs (49%) confirmed in the OCT en face and OCT B-scan images presented with punctate hyperfluorescent spots, characteristic of MAs in IA images. For 25 of the 49 MAs (51%), IA images were available, but matching punctate hyperfluorescent spots were not observed. Furthermore, no statistical correlation

regarding MA lumen closure was observed between the OCTA en face image findings and the FA image findings.

Hyperfluorescent spots indicating MAs on FA images were significantly more common when circinate hard exudates were present around the MA ($P < .001$, Wilcoxon signed rank test).

Nodular-type MAs

Figure 1 shows a representative image of a nodular-type MA. The patient was a 63-year-old man with PDR in the left eye. His logMAR visual acuity was 0.52 and his central macular thickness was 345 μm. Overall, 54 MAs (65%) were of the nodular type. Of these, 40 (74%) were open, 11 (20%) were closed, and 3 (6%) were heterogeneous. Edema was observed in the vicinity of the MA in 42 MAs (78%), but not around 12 MAs (22%). Hyperfluorescent spots were observed in 47 of the 49 nodular-type MAs (96%) for which FA images were available, and in 17 of the 34 MAs (50%) for which IA images were obtained. The mean MA depth was 154.0 μm and the mean maximum diameter was 104.9 μm (Table 1).

Comma-like-type MAs

Figure 2 shows a representative image of a comma-like-type MA, seen in the right eye of the same patient shown in Figure 1. The logMAR visual acuity was 0.15 and the central macular thickness was 320 μm. There were 19 comma-like-type MAs in total (23%). Of these, 15 (79%) were open and 4 (21%) were closed. Edema was observed nearby in 13 MAs (68%), but not in 6 MAs (32%). Hyperfluorescent spots consistent with MAs were observed in 14 (87%) of the 16 comma-like-type MAs for which FA images were available and in 5 (50%) of the 10 comma-like-type MAs for which IA images were obtained. The mean MA depth was 144.3 μm and the mean maximum diameter was 96.4 μm (Table 1).

Table 1 Characteristics per type of microaneurysm visualized by en face OCTA

	Nodular type	Comma-like type	Absent type
Open lumen of the microaneurysm	40/54 (74%)	15/19 (79%)	6/10 (60%)
Retinal edema around the microaneurysm	42/54 (78%)	13/19 (68%)	7/10 (70%)
Hyperfluorescent spots on FA	47/49 (96%)	14/16 (87%)	8/9 (88%)
Hyperfluorescent spots on IA	17/34 (50%)	5/10 (50%)	2/5 (20%)
Maximum diameter of the microaneurysm, μm	154.0	96.4	127.3
Mean (SD) depth of the microaneurysm, μm	104.9 (45.0)	144.3 (35.2)	150.2 (36.4)
Mean (SD) disease duration, mo	25.0 (32.5)	83.8 (32.8)	64.5 (54.8)
Microaneurysm in the deep plexus	45/54 (83%)	19/19 (100%)	10/10 (100%)
Hard exudates	34/54 (62%)	12/19 (63%)	9/10 (90%)

FA fluorescein angiography, IA indocyanine green angiography

No statistically significant difference was found between each type of MA (nodular, comma-like, or absent) and each parameter

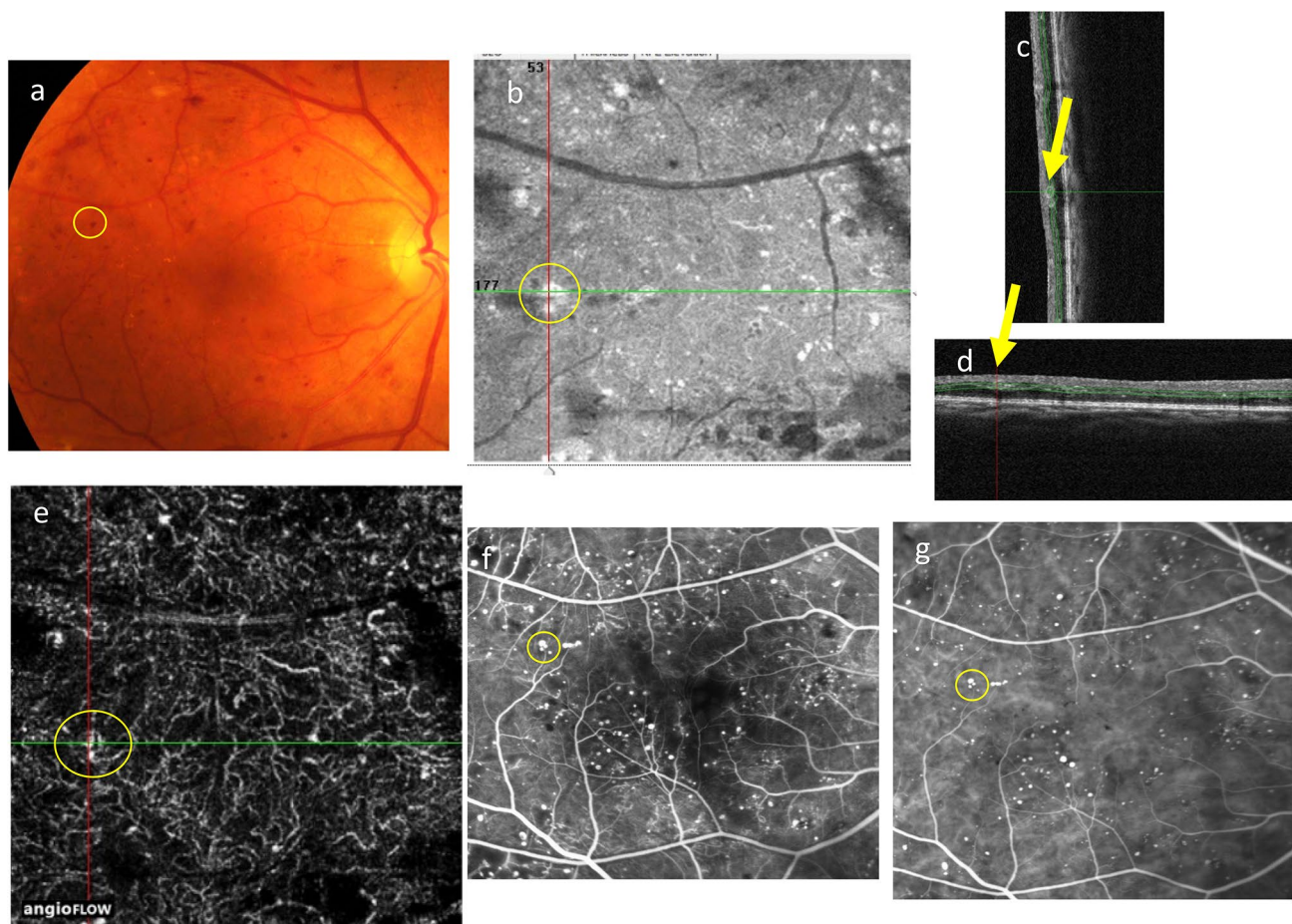


Fig. 2 The patient was a 63-year-old man with PDR of the right eye. **a** A fundus photograph shows a red punctate spot thought to be MA (yellow mark). **b** MA is seen in a 3×3 mm square of an en face image (C-scan image) (yellow mark). The MA was confirmed in B-mode images with the vertical (**c**) and horizontal (**d**) sliders aligned. A ring shape thought to be the MA can be seen. The MA lumen was open and cystoid macular edema was observed in the

vicinity. **e** A comma-like finding was observed in a 3×3 mm square OCTA image (deep prex). This was defined as a comma-like type. **f** The yellow mark shows hyperfluorescence in an FA image (1 minute 6 seconds) matching the OCTA image. **g** The yellow mark shows hyperfluorescence in an IA image (2 minutes 41 seconds) matching the OCTA image

Absent-type MAs

Figure 3 shows a representative image of an absent-type MA. The patient was a 64-year-old woman with moderate NPDR in the left eye. Her logMAR visual acuity was 0.22 and her central macular thickness was $495 \mu\text{m}$. There were 10 absent-type MAs (12%). In the OCT B-scan images, 6 (60%) were open and 4 (40%) were closed. Edema was observed adjacent to 7 MAs (70%), but not around 3 MAs (30%). Hyperfluorescent spots consistent with MAs were observed in 8 (88%) of the 9 absent-types MAs for which FA images were available and in 2 (40%) of the 5 absent-type MAs for which IA images were obtained. The mean

MA depth was $150.2 \mu\text{m}$ and the mean maximum diameter was $127.3 \mu\text{m}$ (Table 1).

Statistical analysis

No significant differences were found between each type of MA (nodular, comma-like, or absent), nor between any of the parameters (Table 1).

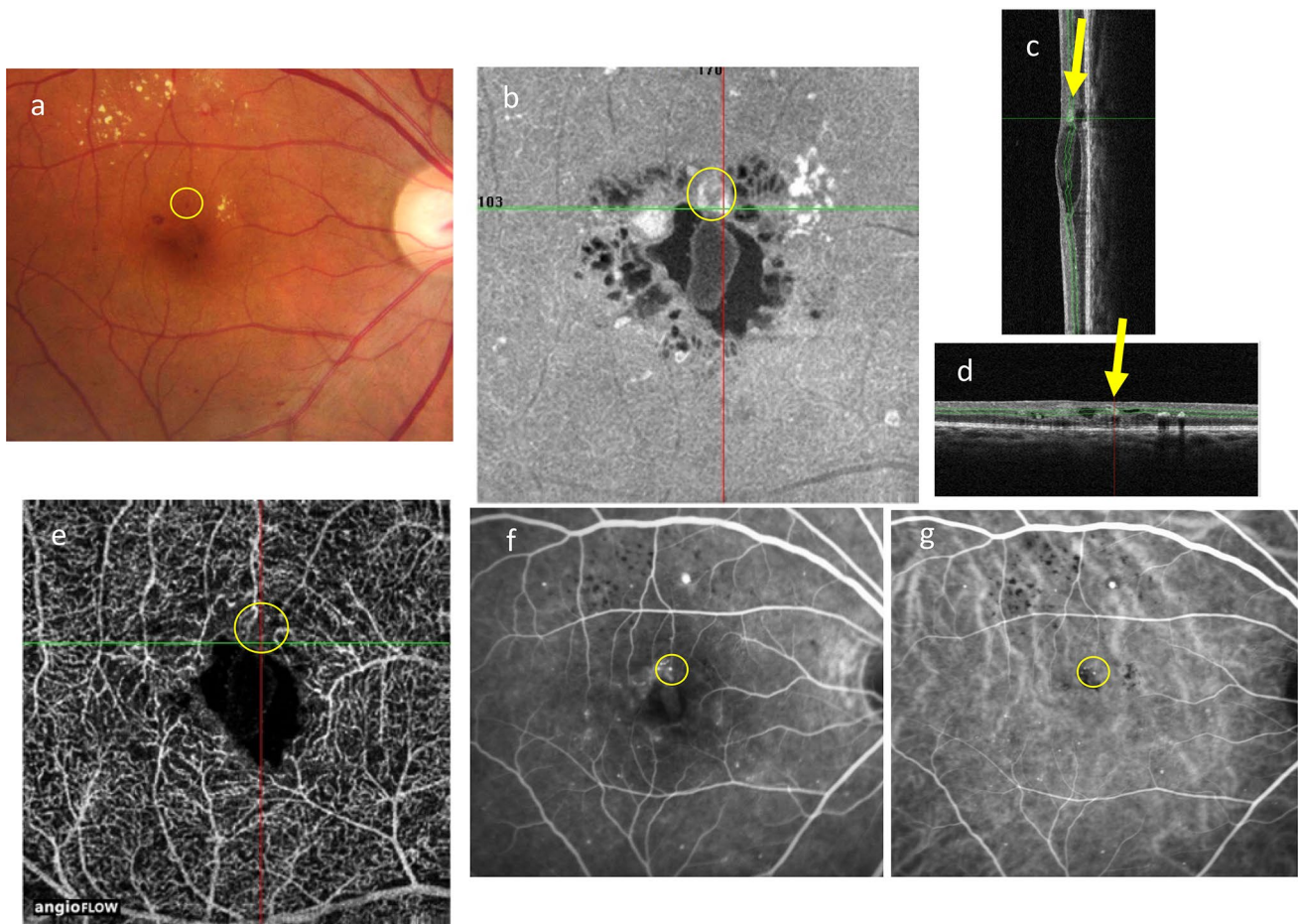


Fig. 3 The patient was a 64-year-old woman with moderate NPDR of the left eye. **a** Fundus photograph shows a red punctate spot thought to be MA (yellow mark). **b** MA is seen in a 3×3 mm square of an en face image (C-scan image) (yellow mark). The MA was confirmed in B-mode images with the vertical (**c**) and horizontal (**d**) sliders aligned. A ring shape thought to be the MA can be seen. The MA

lumen was open and cystoid macular edema was observed in the vicinity. **e** An aneurysm could not be confirmed in a 3×3 mm square OCTA image (deep prex). This was defined as an absent type. **f** The yellow mark shows hyperfluorescence in an FA image (38 seconds) matching the OCTA image. **g** The yellow mark shows hyperfluorescence in an IA image (21 seconds) matching the OCTA image

Discussion

We successfully visualized MAs in DME using OCTA en face images. However, some MAs that were confirmed by OCT B-scan images could not be visualized by OCTA en face images and no vascular signs were detected. In this study, we identified MAs in color pictures and OCT en face images first, and then confirmed those nodular findings in the OCT B-scan slice with the horizontal and vertical sliders aligned at the nodular spots in the OCT en face slice. We defined MAs in OCT B-scan images as findings exhibiting a capsular shape and ring-sign, as reported by Horii colleagues [17]. In total, 83 MAs were found. When these MAs were observed with OCTA en face images, 88% presented with nodular, comma-like, or semilunar findings, considered to represent MAs. However, 12% of

MAs could not be visualized with the AngioVue image. Moreover, hyperfluorescent spots consistent with MAs were observed in 8 (88%) of the 9 absent-type MAs for which FA images were available. Parravano and colleagues [15] also reported that MAs could not be visualized with the AngioVue imaging system. This suggests that there are limitations to observing MAs using OCTA en face images and that combining OCT B-scan, OCT en face, and FA images allows a more accurate imaging of MAs.

In the clinical setting, MAs are generally diagnosed during a fundoscopic examination and documented using color fundus photography. When MAs are treated with laser, FA is performed to confirm the presence of pathologic capillaries, from which dye leakage can be observed. FA provides good capillary images showing pathologic status, such as dye staining or leakage. On the other hand, the OCT B-scan, which provides an image of an MA from another aspect, is

one of the breakthrough tools for visualizing MAs. A combination of OCT B-scan and OCT en face imaging is a useful method for ascertaining the presence of MAs suggested in color pictures or FA and appears to be a superior method for definitively detecting MAs.

OCTA en face imaging gained attention as a groundbreaking diagnostic imaging method that can replace FA. However, this study showed that OCTA en face images have limitations for detecting MAs and that FA or OCT B-scans are still a necessary test in some patients.

Several explanations are possible for why MAs were not depicted by OCTA en face images in the present study. One possibility is the absence of blood flow due to MA closure. However, 60% of absent-type MAs had open lumens in the OCT B-scan images, which contradicts this hypothesis and suggests the existence of MAs with open lumens but without blood flow. Another possibility may be that thickened MA walls are barriers that inhibit the detection of flow signals. Microaneurysms are histologically defined as dilated blood vessels with basal lamina that contain hyaline, fiber, and fat and that show vascular endothelial cell hyperplasia [20]. Thus, MAs with thickened vascular walls may not be detectable using OCTA en face images.

In recent studies on OCTA, MAs were reported to be well depicted with the AngioVue device. In those studies, MAs were defined as hyperfluorescent spots on FA images, and these areas were then matched using OCTA en face images [3]; however, Ishibazawa and colleagues [3] found some discrepancies. Although we defined MAs as hyperfluorescent spots in the early and/or late phases of FA, there was incomplete agreement between MAs shown on FA and those shown on OCTA [3]. Furthermore, Couturier and colleagues found significantly fewer MAs with OCTA en face images than with FA images [16]. They reported that only 62% of the MAs observed by FA could be confirmed with OCTA en face images.

In the present study, we surmised that highly luminescent ring-shaped morphologies in OCT en face images were MAs. We then aligned the horizontal and vertical sliders to these areas and defined MAs as findings in the horizontal and vertical OCT B-scan images presenting with a capsular shape and the ring-sign characteristics of MA, as reported by Horii and colleagues [17]. This is the first report to use this MA definition for comparison with OCTA en face imaging findings, and we believe it to be a highly reliable method of understanding OCTA en face MA images.

We also proposed 3 morphological categories for OCTA en face MA images: nodular type, absent type, and comma-like type. A variety of MA morphologies, including the comma-like, coil-shaped, and semilunar types, were observed with OCTA en face images in the present study. Sitt and colleagues [20] and Moore and colleagues [21] used

trypsin digest preparations of donated eyes to observe MAs by electron microscopy. They reported that MAs morphologically presented as saccular, fusiform, or focal bulges [18, 19]. The variety of OCTA en face images in our study may represent the visual histopathology of MAs. The variety of OCTA en face images may correlate with the variety of histopathologic morphologies of MAs. The saccular and fusiform types may represent the nodular type in OCTA en face images, while the focal bulge morphologies may represent the comma-like type.

Microaneurysms are said to be dynamic capillary defects that spontaneously disappear, with an average 2-year half-life. Tam and colleagues [22] reported adaptive optics scanning laser ophthalmoscope images of MA formation and disappearance and compared these with FA images. They reported that the morphology of MAs changes in various ways, such as capillary protrusion, capillary bulging, and multilobed MAs, from formation to disappearance. The wide variation in OCTA en face MA findings that we observed here is consistent with those of past studies.

About 80% of MAs reportedly form in the inner nuclear layer, with deeper MAs seen on the boundary of the inner and outer layers (deep plexus) [2, 3, 9, 17]. Couturier and colleagues [16] observed 60% of MAs in the deep vascular layer when using OCTA en face images. In the present study, we found 90% of MAs in the deep plexus, which was higher than previously reported [16]. This discrepancy may arise from the definition of MA: in their study, they defined MAs as hot spots in FA.

Conclusions

In this study, circinate hard exudates around MAs correlated with hyperfluorescent spots on FA, but did not correlate with the morphology observed on OCTA. Therefore, while OCTA can help to visualize MA morphology, its findings may not suggest a pathologic state. Therefore, FA is needed to identify the MA targeted for treatment.

The limitations of this study are that it was conducted at a single institution and with a small number of cases. Furthermore, not all MAs were evaluated: only those that could be evaluated with diagnostic imaging were considered.

In conclusion, OCTA en face images can be used to visualize most MAs. However, this finding has to be confirmed with other tools, such as OCT B-scans, en face OCT, and/or FA. Interpretation of OCTA en face images should be clarified in the future.

Conflicts of interest M. Hamada, Equipment (Chuo Sangio); K. Ohkoshi, Equipment (Chuo Sangio); K. Inagaki, Nnoe; N. Ebihara, None; A. Murakami, Grant (Abbott Japan, Alcon Japan, Eisai, HOYA, Kakuen Pharmaceutical, Kowa Pharmaceutical, Lumenis, MSD, Novartis

Phama, Otsuka Pharmaceutical, Pfizer Japan, Santen Pharmaceutical, SEED, Senju Pharmaceutical, Rohto Pharmaceutical, Wakamoto), P (The license for hydrogel ophthalmic lens for gene therapy of eye was acquired by SEED from the Author).

References

- Yeung L, Lima VC, Garcia P, Landa G, Rosen RB. Correlation between spectral domain optical coherence tomography findings and fluorescein angiography patterns in diabetic macular edema. *Ophthalmology*. 2009;116:1158–67.
- Huang Y, Zhang Q, Thorell MR, An L, Durbin MK, Laron M, et al. Swept-source OCT angiography of the retinal vasculature using intensity differentiation-based optical microangiography algorithms. *Ophthalmic Surg Lasers Imaging Retina*. 2014;45:382–9.
- Ishibazawa A, Nagaoka T, Takahashi A, Omae T, Tani T, Sogawa K, et al. Optical coherence tomography angiography in diabetic retinopathy: a prospective pilot study. *Am J Ophthalmol*. 2015;160:35–44.
- Jia Y, Tan O, Tokayer J, Potsaid B, Wang Y, Liu JJ, et al. Split-spectrum amplitude correlation angiography with optical coherence tomography. *Opt Express*. 2012;20:4710–25.
- Jia Y, Bailey ST, Wilson DJ, Tan O, Klein ML, Flaxel CJ, et al. Quantitative optical coherence tomography angiography of choroidal neovascularization in age-related macular degeneration. *Ophthalmology*. 2014;121:1435–44.
- Jia Y, Wei E, Wang X, Zhang X, Morrison JC, Parikh M, et al. Optical coherence tomography angiography of optic disc perfusion in glaucoma. *Ophthalmology*. 2014;121:1322–32.
- Mariampillai A, Standish BA, Moriyama EH, Khurana M, Munce NR, Leung MK, et al. Speckle variance detection of microvasculature using swept-source optical coherence tomography. *Opt Lett*. 2008;33:1530–2.
- Miura M, Makita S, Iwasaki T, Yasuno Y. Three-dimensional visualization of ocular vascular pathology by optical coherence angiography in vivo. *Invest Ophthalmol Vis Sci*. 2011;52:2689–95.
- Miura M, Hong YJ, Yasuno Y, Muramatsu D, Iwasaki T, Goto H. Three-dimensional vascular imaging of proliferative diabetic retinopathy by Doppler optical coherence tomography. *Am J Ophthalmol*. 2015;159:528–38.
- Schwartz DM, Fingler J, Kim DY, Zawadzki RJ, Morse LS, Park SS, et al. Phase-variance optical coherence tomography: a technique for noninvasive angiography. *Ophthalmology*. 2014;121:180–7.
- Spaide RF, Klancnik JM Jr, Cooney MJ. Retinal vascular layers imaged by fluorescein angiography and optical coherence tomography angiography. *JAMA Ophthalmol*. 2015;133:45–50.
- Cheng S, Leng T. Noninvasive detection of microaneurysms in diabetic retinopathy by swept-source optical coherence tomography. *Clin Ophthalmol*. 2016;16:1791–5.
- Miwa Y, Murakami T, Suzuma K, Uji A, Yoshitake S, Fujimoto M, et al. Relationship between functional and structural changes in diabetic vessels in optical coherence tomography angiography. *Sci Rep*. 2016;6:29064.
- Salz DA, de Carlo TE, Adhi M, Moulton E, Choi W, Bauman CR, et al. Select features of diabetic retinopathy on swept-source optical coherence tomographic angiography compared with fluorescein angiography and normal eyes. *JAMA Ophthalmol*. 2016;1:644–50.
- Parravano M, De Geronimo D, Scarinci F, Querques L, Virgili G, Simonetti JM, et al. Relationship between internal reflectivity of diabetic microaneurysms on SD-OCT and detection on OCT angiography. *Am J Ophthalmol*. 2017;179:90–6.
- Couturier A, Mané V, Bonnifant S, Erginay A, Massin P, Gaudric A, et al. Capillary plexus anomalies in diabetic retinopathy on optical coherence tomography angiography. *Retina*. 2015;35:2384–91.
- Horii T, Murakami T, Nishijima K, Sakamoto A, Ota M, Yoshimura N. Optical coherence tomographic characteristic of microaneurysms in diabetic retinopathy. *Am J Ophthalmol*. 2009;150:840–8.
- Hellstedt T, Immonen I. Disappearance and formation rates of microaneurysms in early diabetic retinopathy. *Br J Ophthalmol*. 1996;80:135–9.
- Jalli PY, Hellstedt TJ, Immonen IJ. Early versus late staining of microaneurysms in fluorescein angiography. *Retina*. 1997;17:211–5.
- Stitt AW, Gardiner TA, Archer DB. Histological and ultrastructural investigation of retinal microaneurysm development in diabetic patients. *Br J Ophthalmol*. 1995;79:362–7.
- Moore J, Bagley S, Ireland G, McLeod D, Boulton ME. Three dimensional analysis of microaneurysms in the human diabetic retina. *J Anat*. 1999;194:89–100.
- Tam J, Dhamdhare KP, Tiruveedhula P, et al. Subclinical capillary changes in non-proliferative diabetic retinopathy. *Optom Vis Sci*. 2012;89:E692–703.